

Spinels and other oxides in Mn-rich rocks from the Hutter Mine, Pittsylvania County, Virginia, U.S.A.: Implications for miscibility and solvus relations among jacobsite, galaxite, and magnetite

JAMES S. BEARD^{1,*} AND ROBERT J. TRACY²

¹Virginia Museum of Natural History, 1001 Douglas Avenue, Martinsville, Virginia 24112, U.S.A.

²Department of Geological Sciences, Virginia Polytechnic Institute and State University, Blacksburg, Virginia 24061, U.S.A.

ABSTRACT

The Hutter Mine locality, Pittsylvania County, Virginia, is a metamorphosed magnetite deposit, with substantial development of subsidiary manganite marble, that occurs within Latest Precambrian or Early Paleozoic sillimanite-grade pelitic schists. Manganese oxides and spinels at the Hutter Mine include manganosite (MnO) (coexisting with hausmannite and jacobsite) as well as spinels rich in jacobsite (FeMn₂O₄), magnetite (Fe₃O₄), and galaxite (MnAl₂O₄), and a variety of intermediate solid solutions between these three end-members. Several samples contain spinels that exhibit substantial miscibility along the jacobsite-galaxite and jacobsite-magnetite joins. Magnetite-galaxite solid solution is, by comparison, very limited. Coexisting manganite spinels within the jacobsite-galaxite-magnetite ternary system include jacobsite-rich varieties with galaxite <65 (normalized to glx + mag + jac = 100) that coexist with Mg-Zn-bearing galaxite-rich spinel with galaxite >75. However, the wide range of spinel compositions at the Hutter Mine largely reflects compositional variability in the host rock. In a skarn reaction zone between Fe-rich, quartz-bearing amphibolites and Si-poor, Mn-rich marbles, the galaxite content of spinel drops from 60% to near zero as silica activity increases over a 5 mm interval. In this same reaction zone, magnetite content of spinel increases from about 10 to 95%, but over a narrower interval (about 2 mm). Total variation in spinel composition in this reaction zone is nearly the same as that seen over the entire suite of Hutter Mine samples.

Both regional metamorphic geology and thermobarometry on local pelite samples indicates that T_{\max} at the Hutter Mine was 550–600 °C. Manganite formed by the decarbonation of Mn-rich carbonate in the presence of a CO₂-poor ($X_{\text{CO}_2} \leq 0.01$) fluid having $\log a_{\text{SiO}_2} < -3.0$. Oxygen fugacity in the manganite-bearing sample was buffered by coexisting manganite and hausmannite, placing f_{O_2} within the magnetite stability field at peak T . This result is consistent with the occurrence of magnetite as the principal ore at Hutter.

The extensive miscibility observed along the jacobsite-galaxite join requires reexamination of miscibility gaps proposed in previous studies. We suggest that the wide compositional gaps found in previous studies reflect a variety of chemical factors of which silica activity is the most critical. In particular, the large range of silica activities observed in Hutter Mine rocks stabilizes spinels with a wide range in galaxite content. The crests of both the jacobsite-galaxite and jacobsite-magnetite two-phase regions appear to occur at relatively low temperatures, probably below 600 °C.

INTRODUCTION

Manganese-oxide minerals are important both economically and as petrogenetic indicators. The major ores of manganese are all oxides and hydroxides. Because Mn occurs in three different valence states, Mn oxides can be useful indicators of oxygen fugacity. Among Mn-spinels, jacobite (jac, MnFe³⁺O₄) is an important ore mineral (e.g., Dasgupta et al. 1990). Its aluminate analog, galaxite (glx, MnAl₂O₄), is much rarer. Both are largely normal spinels (Hill et al. 1979). Limited experimental work as well as studies of natural assemblages containing coexisting jac- and glx-rich spinels have suggested substantial immiscibility at temperatures below 800–900 °C (Essene and Peacor 1983; Ishida et al. 1977), similar to other

aluminate-ferrite pairs (e.g., Carvalho and Sclar 1988; Lindsley 1991; Ghiorso and Sack 1991). Although we are aware of no studies of jac-magnetite (mag) solid solutions, the normal to inverse transition that must occur along this join would also seem to favor significant low-temperature immiscibility (e.g., Lindsley 1991). Nonetheless, our compositional data on the naturally occurring Mn-Al-Fe spinel suite at the Hutter Mine indicates substantial, possibly complete, miscibility along both the jac-glx and jac-mag joins at temperatures of 600 °C or less.

GEOLOGIC SETTING

The Hutter Mine is located near the town of Pittsville, in northern Pittsylvania County in south-central Virginia, about 3 km southeast of the northwestern margin of the Smith River Allochthon (SRA; Fig. 1). This margin is a Paleozoic thrust fault with high-grade (amphibolite to, locally, granulite facies)

* E-mail: jbeard@vmnh.org

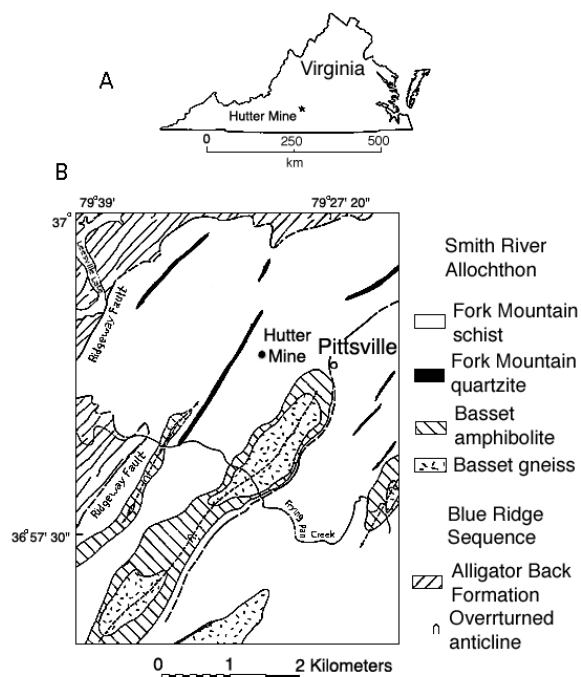


FIGURE 1. (A) Location of the Hutter Mine in south-central Virginia. (B) Geology in the vicinity of the Hutter Mine.

rocks of the SRA thrust westward over lower-grade (greenschist and lower-amphibolite facies) rocks of the Blue Ridge Province (Espenshade 1954; Conley and Henika 1973; Glover et al. 1983; Marr 1984; Conley 1985; Gates and Speer 1991). The SRA consists of the Fork Mountain Formation (pelitic gneisses and schists with minor quartzite and marble) and the Basset Formation (amphibolite and granitic gneiss). The Hutter Mine lies within a tight, overturned syncline in Fork Mountain schist that is sandwiched between overturned anticlines cored by Basset amphibolites and gneisses (Marr 1984) (Fig. 1). Nearby pelites contain fibrolite, muscovite, staurolite, and garnet, consistent with middle-amphibolite-facies metamorphism.

The principal ore at the Hutter Mine was magnetite. The mine operated for about 25 years, ending around 1903. Descriptions of nearby workings along strike with the Hutter Mine (Watson 1907) suggest that the ore body was a seam of magnetite sandwiched between schist and marble. In these workings, a thin Mn-rich umber separated the marble from the Fe-ore. The spoil heaps at the Hutter Mine contain abundant fragments of schist, marble, quartzite, and amphibolite, consistent with the known association of Mn and Fe mineralization of quartzites and marbles elsewhere in the area (Watson 1907; Furcron 1935; Espenshade 1954; Marr 1984).

OCCURRENCE OF THE MN-RICH ROCKS

Most of the manganese-rich rocks at the Hutter Mine were found in a single, small dump covering an area of perhaps 100 m². The rocks are covered with a blue-black sooty layer of Mn-oxides, but are quite fresh beneath this thin weathering crust. The Mn-rich samples are heterogeneous, consisting of carbon-

ate and oxide-rich layers and lenses, several of which may occur within a single hand specimen. These layers and lenses appear to largely reflect reaction zones rather than original compositional layering (see below). In a few larger samples, reaction zones can be seen between marble and a garnet amphibolite skarn, with an oxide-rich layer next to the marble, followed by a garnet-rich, quartz-bearing layer that then grades into the quartz-bearing garnet amphibolite. Samples of the magnetite ore exploited at the Hutter Mine are surprisingly rare, although a few magnetite-rich samples occur in association with the garnet amphibolites.

We recognize three occurrences of Mn-spinels and-oxides, and other Mn-minerals, from the Hutter Mine samples. (1) marbles containing Mn-spinels and Mn-olivinoids that grade into spinel-olivinoid rocks containing minor carbonate. (2) A single large sample (VMNH no. 598) consisting mostly of the rare Mn-oxide manganosite (MnO) and its alteration products, along with lesser amounts of Mn-Ca carbonates, jacobsonite, hausmannite, and Mn-olivinoids. (3) Specialized assemblages that are limited to reaction zones between Mn-rich rocks and garnet- and quartz-bearing country rocks. All quartz-bearing rocks examined so far are poor in Mn, and the spinels in the country rock are essentially pure magnetite.

PETROGRAPHY AND MINERAL CHEMISTRY

Microprobe analytical procedure and formula recalculation

All mineral analyses were done at Virginia Tech using the Cameca SX50 electron probe microanalyzer. Analytical conditions were 15 kV accelerating potential and 20 nA beam current on brass. Excitation spot size of about 1 μm was typically used. Analyses were corrected using the PAP correction procedure (Pouchou and Pichoir 1985).

Standards used were simple oxides as much as possible (Al₂O₃, Fe₂O₃, TiO₂). Alternatively, metals (Zn) or more complex oxides (Benson orthoclase for Si, Marjalahti olivine for Mg) were used. Manganese proved to be analytically problematic in this study using the normal Mn standard MnO₂, because of very high MnO concentrations, so a natural manganosite crystal from Hutter (with 98.8 wt% MnO, 1.2 wt% FeO) was developed as a standard and worked well.

Spinel structural formulas have been recalculated with all Mn as Mn²⁺ unless required by stoichiometry. For end-member contents specified in the tables, arbitrary end-member assignment is as follows, in this order: (1) all Fe²⁺ to magnetite; (2) the remaining Fe³⁺ to jacobsonite, and (3) the remaining Mn to galaxite. All galaxite, jacobsonite, and magnetite contents reported in this paper refer to values of each end-member normalized to 100% jac + glx + mag.

Manganosite and coexisting oxide minerals

Manganosite and its alteration products constitute about 50–60% by mode of a single large sample (5 kg) from the Hutter Mine (VMNH no. 598). In hand sample, the manganosite is largely obscured by abundant sooty alteration products. In thin section, however, it is a brilliant green, isotropic mineral. Manganosite (99 wt% MnO end-member, with about 1 wt% FeO) occurs with two other primary oxide minerals: jacobsonite (up to 96 mol% of the MnFe₃³⁺O₄ end-member) and hausmannite

(99 mol% of the $Mn^{2+}Mn_2^{3+}O_4$ end-member) (Table 1). Hausmannite and jacobite occur as 1–5 mm, rounded opaque grains, locally in contact with each other and with manganosite. Other minerals in this sample include Mn-Ca carbonate ($Ca_{15}Rds_{45}$), Mn-humite minerals, alabandite, and manganosphenite. All mineral abbreviations are according to Kretz (1983), except for rare minerals not in his list for which we specify abbreviations here.

Manganosite is an exceptionally rare mineral. Pyrochroite derived from manganosite is a major ore of Mn in the Noda-Tamagawa district of Japan, where manganosite has been interpreted to have formed by metamorphic decarbonation of rhodochrosite (Watanabe et al. 1970). Manganosite is present in small quantities in the Zn deposits at Franklin, New Jersey and in the Fe-Mn deposits of Långban, Sweden (Huebner 1969; McSween 1976).

Spinel

Mn-Fe-Al spinels are common to abundant in all Mn-rich rocks from the Hutter Mine. The spinels range from pure magnetite in the quartz-bearing rocks, to >95% jacobite (jac, $MnFe_2O_4$) and to >80% galaxite (glx, $MnAl_2O_4$) (Tables 1 and 2). The Fe-rich spinels are opaque, but crystals with as little as 20 mol% galaxite component may be a translucent red-brown at thin edges. Hutter Mine spinels are strongly magnetic and can be separated from crushed samples of the rock with a hand magnet. In the marbles, spinels usually occur as isolated

rounded grains that may range up to 2–3 mm in diameter. Although discrete crystals of spinel also occur in the spinel-silicate rocks, they are also common as complex, symplectic (“fingerprint”) intergrowths with Mn-humite minerals. Some marbles are spotted with “blooms” of these intergrowths a centimeter or more across.

There is extensive solid solution between jacobite and magnetite, and between jacobite and galaxite in the Hutter Mine rocks (Fig. 2). Hutter Mine spinels contain >95 mol% jac + glx + mag. However, a few Fe-rich spinels may have 5–8% ulvospinel component, and the most aluminous spinels (glx > 75) commonly have 5–16% gahnite ($ZnAl_2O_4$) plus spinel ($MgAl_2O_4$) (Table 2). These Al-Mg-Zn-rich spinels occur in low abundances as a second spinel in many samples. Petrographically they occur as small, anhedral grains at the margins of, interstitial to, or partially mantling the main spinel phase. In several samples, an Fe-rich third spinel phase occurs together with the Al-rich spinel (Table 2; Fig. 3). These late spinels (the examples shown in Fig. 3 are plotted separately on Fig. 2) may either be retrograde, subsolvus spinels or recrystallized exsolutions from the main spinel phase. Nevertheless, most of the wide range in spinel compositions at the Hutter Mine, even within individual samples, is apparently related to local bulk compositional heterogeneities (differences between carbonate- and silicate-rich areas in heterogeneous samples or variations within reaction zones). We have found no examples of either jacobite-rich or galaxite-rich spinels coexisting with magnetite-rich spinels.

Several described metamorphosed Mn-oxide deposits contain coexisting jac- and glx-rich spinels. For example, at the amphibolite-facies Bald Knob (North Carolina) deposit, the jac-glx miscibility gap extends from glx_{20} to glx_{80} (Essene and

TABLE 1. Coexisting Mn-(Fe) oxides, Sample VMNH no. 598

| | Jacobite | | | | Hausmannite | Manganosite | high Fe | avg. |
|--------------------------------|----------|--------|---------|-------|-------------|-------------|---------|--------|
| | low Al | | high Al | | | | | |
| | rim | inter | core | avg. | | | | |
| SiO ₂ | 0.05 | 0.02 | 0.03 | 0.04 | 0.04 | 0.03 | 0.03 | 0.03 |
| TiO | 0.00 | 0.00 | 0.40 | 0.13 | 0.03 | 0.02 | 0.01 | 0.01 |
| Al ₂ O ₃ | 0.01 | 1.85 | 6.80 | 3.13 | 0.00 | 0.01 | 0.01 | 0.01 |
| MgO | 0.23 | 0.24 | 0.35 | 0.27 | 0.09 | 0.08 | 0.21 | 0.20 |
| MnO | 30.06 | 30.55 | 31.64 | 30.72 | 31.00 | 31.11 | 99.25 | 99.10 |
| Mn ₂ O ₃ | 1.08 | 0.99 | 1.84 | 0.69 | 68.58 | 69.27 | 0.00 | 0.00 |
| FeO | 0.00 | 0.00 | 0.00 | 0.00 | 0.00 | 0.00 | 0.94 | 0.78 |
| Fe ₂ O ₃ | 67.80 | 66.12 | 59.03 | 64.44 | 0.43 | 0.11 | 0.00 | 0.00 |
| ZnO | 0.31 | 0.23 | 0.38 | 0.29 | 0.00 | 0.05 | 0.06 | 0.10 |
| sum | 99.54 | 100.00 | 100.47 | 99.71 | 100.17 | 100.66 | 100.51 | 100.22 |

| | Formula proportions* | | | | | | | |
|------------------|----------------------|-------|-------|-------|-------|-------|-------|-------|
| Fe ³⁺ | 1.964 | 1.887 | 1.630 | 1.831 | 0.012 | 0.003 | 0.000 | 0.000 |
| Fe ²⁺ | 0.000 | 0.000 | 0.000 | 0.000 | 0.000 | 0.000 | 0.009 | 0.008 |
| Si | 0.002 | 0.001 | 0.001 | 0.001 | 0.002 | 0.001 | 0.000 | 0.000 |
| Ti | 0.000 | 0.000 | 0.011 | 0.004 | 0.001 | 0.001 | 0.000 | 0.000 |
| Al | 0.000 | 0.083 | 0.294 | 0.139 | 0.000 | 0.000 | 0.000 | 0.000 |
| Mg | 0.013 | 0.014 | 0.019 | 0.015 | 0.005 | 0.004 | 0.004 | 0.004 |
| Mn ²⁺ | 0.980 | 0.981 | 0.983 | 0.982 | 0.997 | 0.996 | 0.986 | 0.987 |
| Mn ³⁺ | 0.032 | 0.029 | 0.052 | 0.020 | 1.983 | 1.993 | 0.000 | 0.000 |
| Zn | 0.009 | 0.006 | 0.010 | 0.008 | 0.000 | 0.001 | 0.001 | 0.001 |

| | | | | | | |
|-----|-------|------|------|------|-----|-----|
| jac | 100.0 | 96.4 | 85.6 | 93.7 | 0.6 | 0.2 |
| glx | 0.0 | 3.6 | 14.4 | 6.3 | 0.0 | 0.0 |
| mag | 0.0 | 0.0 | 0.0 | 0.0 | 0.0 | 0.0 |

| | | | | | | |
|-------------|-----|-----|-----|-----|------|------|
| haus | 1.6 | 1.4 | 2.6 | 1.0 | 99.1 | 99.7 |
| manganosite | | | | | 98.6 | 98.7 |

Notes: Fe and Mn oxidation by stoichiometry. Calculations assume all Mn²⁺ unless required by charge balance. Jac+glx+mag in spinel (but not hausmannite) normalized to 100%.

* Based on three cations and four oxygen atoms for jacobite and hausmannite, one cation and one oxygen atom for manganosite.

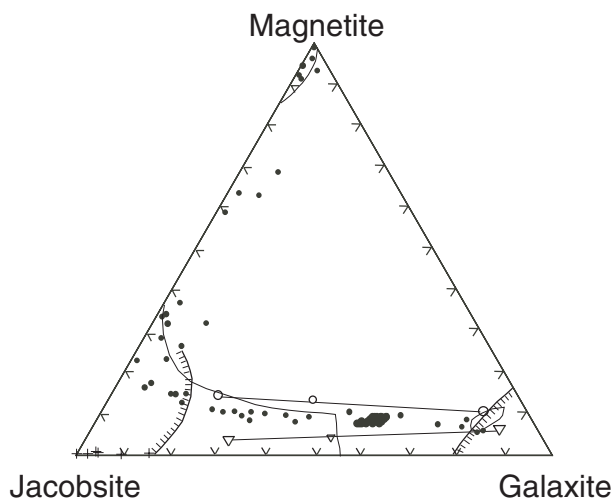


FIGURE 2. Triangular plot of mag-jac-glx. Filled circles are analyses from the VMNH no. 615 reaction zone. Crosses are spinels coexisting with manganosite and hausmannite (VMNH no. 598). Open circles are coexisting exsolved spinels from the aluminous core of a zoned spinel (VMNH no. 603; Table 3). Open triangles are late spinels (VMNH no. 608; Fig. 3). Solid lines outline the compositions of spinels from all other Hutter Mine samples. Hatchured lines mark the limits of spinel compositions reported from Bald Knob (Essene and Peacor 1983).

TABLE 2. Selected Spinel Analyses, Hutter Mine

| VMNH sample no. | 615 (reaction zone) | | | 608 | | | late Al-rich | late Fe-rich | 591 | 613 | 616 | 612 | 596 |
|--------------------------------|------------------------|--------|-------|--------|--------|--------|-----------------|-----------------|-------|-------|--------|--------|-----|
| SiO ₂ | 0.00 | 0.09 | 0.08 | 0.02 | 0.01 | 0.01 | 0.01 | 0.01 | 0.02 | 0.04 | 0.02 | | |
| TiO ₂ | 0.55 | 0.97 | 0.27 | 0.26 | 0.12 | 0.03 | 0.21 | 0.81 | 0.09 | 0.41 | 0.17 | 0.01 | |
| Al ₂ O ₃ | 2.98 | 3.85 | 0.05 | 31.60 | 27.76 | 51.76 | 15.58 | 10.50 | 1.22 | 3.08 | 0.20 | 0.08 | |
| MgO | 0.06 | 0.17 | 0.01 | 0.40 | 0.71 | 2.72 | 0.32 | 0.42 | 0.21 | 0.28 | 0.01 | 0.03 | |
| CaO | 0.25 | 0.32 | 0.25 | | | | | 0.02 | 0.00 | 0.06 | | | |
| MnO | 11.99 | 23.83 | 2.30 | 32.52 | 32.93 | 31.15 | 31.59 | 30.87 | 23.72 | 29.94 | 3.16 | 0.05 | |
| FeO | 19.98 | 8.44 | 28.47 | 3.11 | 1.36 | 1.54 | 1.32 | 1.34 | 6.53 | 1.12 | 28.29 | 31.10 | |
| Fe ₂ O ₃ | 65.48 | 63.74 | 67.62 | 31.91 | 37.21 | 10.48 | 50.40 | 54.93 | 66.67 | 64.73 | 69.13 | 69.52 | |
| ZnO | 0.00 | 0.08 | 0.00 | 0.45 | 0.66 | 3.78 | 0.20 | 0.29 | 0.23 | 0.08 | 0.05 | 0.17 | |
| sum | 101.29 | 101.50 | 99.04 | 100.27 | 100.74 | 101.46 | 99.63 | 99.20 | 98.71 | 99.73 | 101.01 | 100.95 | |
| Formula proportions* | | | | | | | | | | | | | |
| Fe ³⁺ | 1.838 | 1.772 | 1.976 | 0.778 | 0.919 | 0.229 | 1.340 | 1.504 | 1.936 | 1.838 | 1.981 | 1.996 | |
| Fe ²⁺ | 0.623 | 0.261 | 0.924 | 0.084 | 0.037 | 0.037 | 0.039 | 0.041 | 0.211 | 0.035 | 0.901 | 0.992 | |
| Si | 0.000 | 0.003 | 0.003 | 0.001 | 0.000 | 0.000 | 0.000 | 0.001 | 0.002 | 0.001 | 0.000 | 0.000 | |
| Ti | 0.015 | 0.027 | 0.008 | 0.006 | 0.003 | 0.001 | 0.006 | 0.022 | 0.003 | 0.012 | 0.005 | 0.000 | |
| Al | 0.131 | 0.168 | 0.002 | 1.208 | 1.074 | 1.769 | 0.649 | 0.450 | 0.055 | 0.137 | 0.009 | 0.004 | |
| Mg | 0.003 | 0.009 | 0.001 | 0.019 | 0.035 | 0.118 | 0.017 | 0.023 | 0.012 | 0.016 | 0.001 | 0.002 | |
| Ca | 0.010 | 0.013 | 0.010 | 0.000 | 0.000 | 0.000 | 0.000 | 0.001 | 0.000 | 0.002 | 0.000 | 0.000 | |
| Mn | 0.379 | 0.745 | 0.076 | 0.893 | 0.915 | 0.765 | 0.945 | 0.951 | 0.775 | 0.956 | 0.102 | 0.002 | |
| Zn | 0.000 | 0.002 | 0.000 | 0.011 | 0.016 | 0.081 | 0.005 | 0.008 | 0.007 | 0.002 | 0.001 | 0.005 | |
| jac | 30.0 | 64.6 | 6.4 | 31.2 | 44.3 | 9.6 | 64.1 | 73.4 | 76.9 | 89.7 | 9.0 | 0.4 | |
| glx | 6.7 | 8.4 | 0.1 | 60.2 | 51.7 | 85.8 | 31.9 | 22.4 | 1.8 | 6.7 | 0.3 | 0.0 | |
| mag | 63.3 | 27.0 | 93.5 | 8.6 | 3.9 | 4.7 | 4.0 | 4.2 | 21.4 | 3.6 | 90.7 | 99.6 | |

Notes: Fe and Mn oxidation by stoichiometry. Calculations assume all Mn²⁺ unless required by stoichiometry. Jac, glx, and mag normalized to 100%
 * Based on three cations and four oxygen atoms

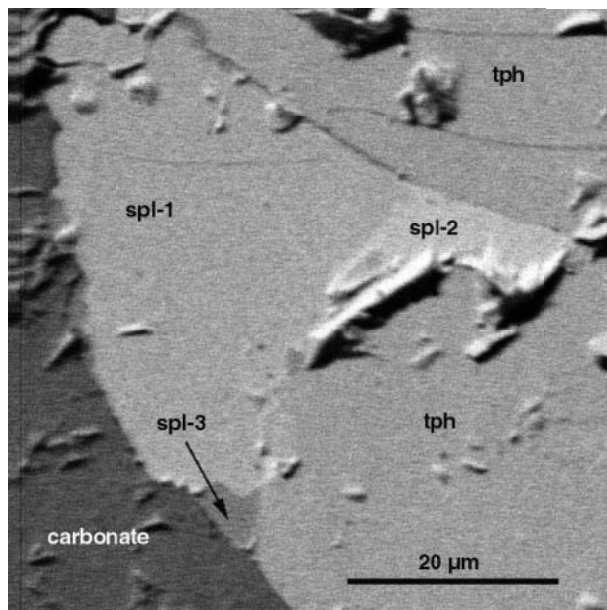


FIGURE 3. BSE image of coexisting spinels from VMNH no. 608. Compositions given in Table 2. Bright Fe-rich and dark Al-rich spinels are marginal to and locally interstitial to the main, moderately aluminous spinel phase (medium gray). Image is ~60 mm across.

Peacor 1983), a region of compositional space that is almost fully occupied by the Hutter Mine spinels (Fig. 2). When aluminous spinels known to be stable at Bald Knob are considered along with Hutter Mine spinels, the only permitted miscibility gap is narrow and highly asymmetric (i.e., between glx₇₅ and glx₆₅; Fig. 2).

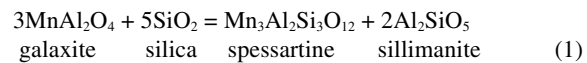
The extensive miscibility between jacobite and magnetite

reflects, in part, the occurrence of manganoan magnetite and ferroan Mn-spinel in a number of samples. However, the only magnetites with jac_{>15} or jacobites with mag_{>40} occur in a narrow (<3 mm) reaction zone in a single sample (see below). We found no spinels with jac₄₅₋₆₀ along the jac-mag join (Fig. 2). Flohr (1992) reports manganoan magnetite (approximately mag₆₀jac₄₀) from the Bald Knob locality, but no context was given.

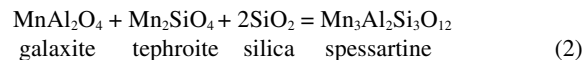
Spinel compositional variation in reaction zones

The effects of bulk composition and reaction stoichiometry on spinel chemistry are particularly apparent in reaction zones. These zones formed at the interface between strongly silica-undersaturated Mn-humite-bearing marbles and quartz-bearing garnet amphibolites. Figure 4 shows the variation in spinel chemistry across one of these reaction zones in one sample (VMNH no. 615). The points plotted on the figure represent analyses of individual small, mostly unzoned grains, and do not reflect zoning in a single grain or series of grains.

As was shown by Essene and Peacor (1983), galaxite is unstable in the presence of quartz, reacting to form spessartine via the reactions:



or



or similar reactions. In VMNH no. 615, spinel compositions change abruptly from jac₃₀glx₆₀mag₁₀ to jac₆₀glx₃₀mag₁₀ at the first appearance of garnet in the reaction zone (some relict cores of aluminous spinel are preserved near the garnet-in boundary). Within the first mm of the reaction zone, tephroite and

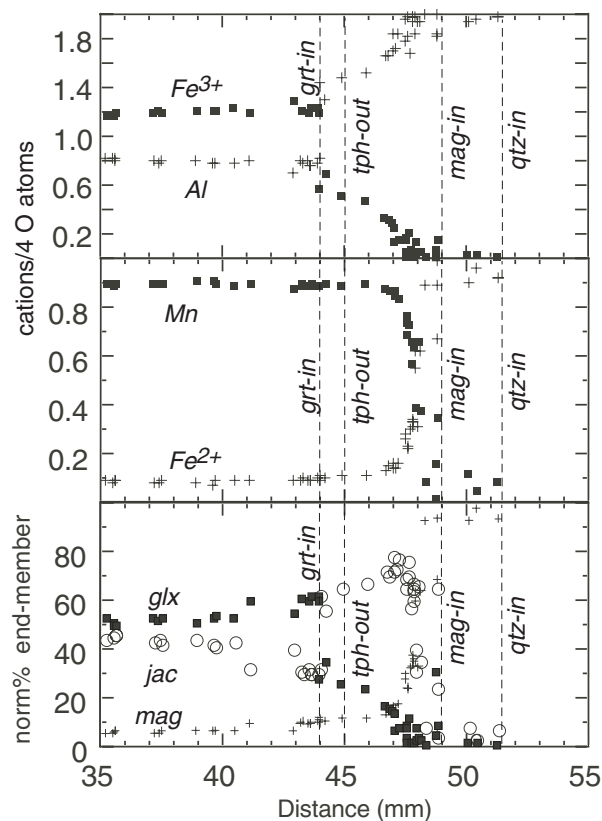


FIGURE 4. Variations in spinel composition across the reaction zone in sample VMNH no. 615. Distances in millimeters. **(Top)** Al and Fe^{3+} . **(Middle)** Mn and Fe^{2+} . **(Bottom)** spinel components glx, jac, and mag. All phases labeled in and out appear or disappear to the right of the plotted dashed lines.

spessartine coexist but tephroite disappears within 1 mm of the spessartine-in boundary, suggesting that reaction 2 initially operated. On the silica-rich side of the spessartine-in boundary, the galaxite content of the spinel decreases monotonically to near zero over a 5 mm interval (Fig. 4top), almost certainly in response to increased silica activity in the reaction zone.

A second compositional variable also affects spinel chemistry in the VMNH no. 615 reaction zone: the relative abundances of Fe and Mn. Garnets in the garnet-quartz amphibolites are almandine-grossular solid solutions with minor (3–8%) spessartine component. Spinels in this rock are essentially pure magnetite. The transition from spinel with about 90 mol% jac + glx to spinel with about 90 mol% mag occurs over an interval of only 1–2 mm, and is much more abrupt than the mineralogical changes associated with increasing silica activity (Fig. 4). It is only within this narrow transition zone that the intermediate jac-mag spinels (see Fig. 2) are found.

The interactions between spinel compositional variation generated by Si activity on the one hand, and by Fe activity on the other, produced some peculiar compositional variations in reaction zone spinels. In particular, the jacobsite content of the spinel at first increases (as galaxite decreases) then drops abruptly (as magnetite increases; Fig. 4). This variation suggests that Si and Fe in the reaction zone behaved differently, likely reflecting differing mechanisms of chemical redistribution.

Zoned and exsolved spinels

In a second reaction zone sample (VMNH no. 603), a replacive reaction front has developed. In this sample, a spinel- and Mn-humite-bearing marble is being replaced by a spessartine-tephroite-spinel skarn (the skarn also contains kinoshitalite, Ba-rich phlogopite) along a knife-sharp front. Spinels in the marble are galaxite-rich. Throughout the skarn, however, most spinels are strongly zoned with relatively homogeneous aluminous cores ($jac_{45}glx_{45}mag_{10}$) and continuously zoned Fe-rich rims ($jac_{60-80}glx_{25-5}mag_{15}$, with Al decreasing outward). The boundary between core and rim is abrupt, with galaxite content dropping from 44 to 22 mol% and jacobsite content increasing from 45 to 65 mol% within <4 μm (Figs. 5 and 6). We interpret this zoning as analogous, in part, to the spinel compositional variations seen in VMNH no. 615. The abrupt compositional change from core to rim likely reflects the onset of reaction to form spessartine component in the skarn. Similarly, the continuous zoning of the rims reflects a continuous increase in silica activity as the reaction front passed. The Mn-Fe zoning, which appears to be mediated by solid-state diffusion in VMNH no. 615, is absent in VMNH no. 603 spinels.

Exsolution has occurred in the aluminous cores of many of the zoned spinels. One typical example from sample VMNH no. 603 is shown in the BSE image in Figure 5. This complexly zoned and exsolved spinel has a diameter of about 120 μm and consists of an aluminous core ($jac_{45}glx_{44}mag_{11}$; dark in the BSE image) surrounded by an Fe-rich mantle (brighter in the BSE image). As noted above, the boundary between core and rim is quite sharp, with essentially constant (except for local, exsolution-related inhomogeneities) galaxite content across the core and monotonically decreasing galaxite content in the mantling ferrite (glx_{22} at the core-mantle boundary decreasing to glx_8 at the outer grain edge) (Fig. 6).

Exsolution or decomposition of the aluminous core is reflected by the roughly circular blebs or spots seen in Figure 5. Each of these consists of a central granule of Al-rich spinel (average $jac_9glx_{80}mag_{11}$) surrounded by a ferrite halo of variable thickness (average $jac_{60}glx_{25}mag_{15}$) (Table 3, also plotted separately on Fig. 2). To discriminate between post-growth exsolution and syn-growth inclusion formation as an explanation for this texture, we performed image analysis on the BSE image in Figure 5 to attempt to integrate Al-rich granules and ferrite haloes to compare with the average composition of the host spinel. In the analysis of all granule-halo pairs in Figure 5, granules averaged 26.8% by area of the total exsolution blebs and haloes 73.2%. We reconstructed the composition of the original spinel using these proportions and the average compositions of granules and haloes determined by electron microprobe. Except for some expected discrepancy among minor elements, the reconstructed compositions closely approximate the composition of the host spinel (Table 3). On this basis, we argue that the granule-halo pairs in the blebs have resulted from binodal or spinodal decomposition of the intermediate spinel composition in the aluminous core of the grain. The average (normalized to the mag-free, jac-glx join) granule composition is 83.4 mol% galaxite and 16.6 mol% jacobsite, compared to an average halo composition of 25.8 mol% galaxite and 74.2

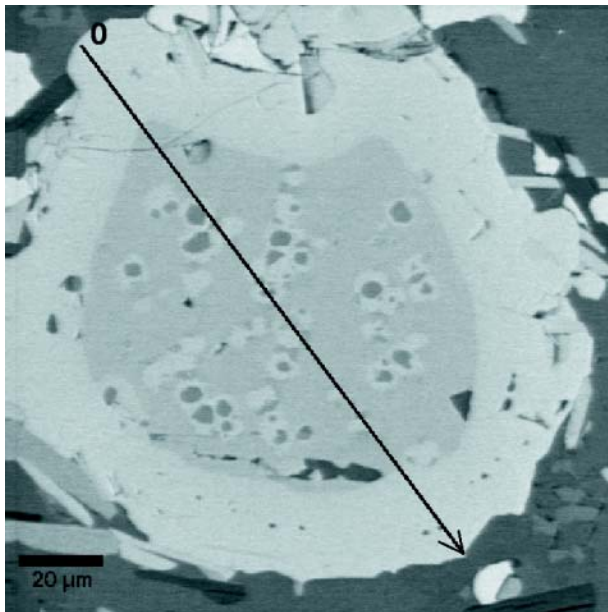


FIGURE 5. BSE image of zoned spinel from VMNH no. 603. Medium-gray core is aluminous spinel, bright rim is Fe-rich. The dark granules surrounded by bright haloes in the core are exsolution features that can be recombined to reproduce the composition of the host spinel. See text and Table 3. Line shows location of the microprobe traverse plotted in Figure 6.

mol% jacobsite, indicating only a mildly asymmetrical miscibility gap in and near this join (Fig. 2).

PHYSICAL AND CHEMICAL CONDITIONS

Conditions of metamorphism

The regional metamorphism of this part of the Smith River Allochthon at mid- to upper-amphibolite-facies conditions has been well established previously (Glover et al. 1983; Conley 1985; Gates and Speer 1991; Henika et al. 2000). In the immediate vicinity of the Hutter Mine locality, mineral assemblages in metapelites are typically qtz-ms-plg-st-grt-bt-sil-gr-ilmm-po (with andalusite in some samples), and assemblages in metabasites are plg-hbl-mag-ilmm (never including pyroxene). Although some higher-grade rocks (sil-kfs-grt-crd in pelites, hbl-cpx-grt in amphibolites) have been described in contact-metamorphic settings from the SRA adjacent to post-regional metamorphic gabbroic plutons, no such plutons have been described within 10 km of the Hutter Mine.

Very fresh samples of pelitic schist have been collected from the dumps at the Hutter Mine. They presumably represent country rock of the deposit that was excavated underground during mining activity and should therefore yield thermobarometric results representing local conditions of metamorphism of the deposit. An analyzed sample (VMNH no. 592) contains the assemblage qtz-plg-ms-bt-chl-sil-tur-gr-ilmm-po. The sample also contains 1 or 2 modal percent of a blocky pleochroic blue-green mineral that was initially suspected to be chloritoid but in fact turned out upon microprobe analysis to be aluminoferro-

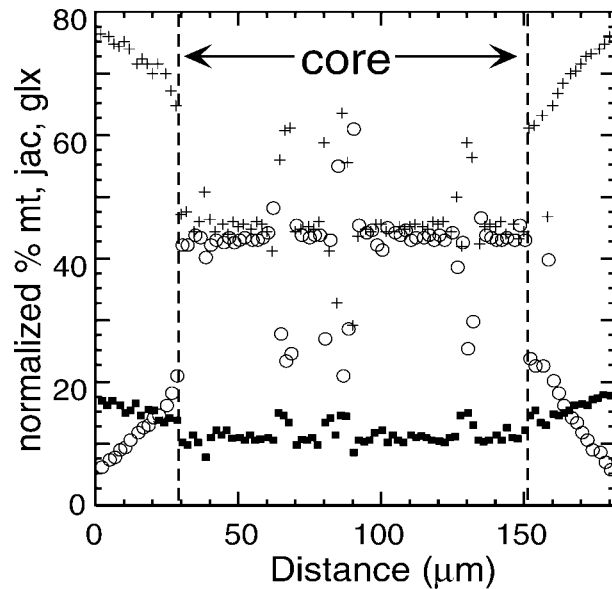


FIGURE 6. Zoning profile across zoned grain from Figure 5 (VMNH no. 603). Inhomogeneities in the interior of the grain represent very fine, late-stage, Al-rich exsolutions surrounded by Fe-rich haloes. Note the discontinuity between core and rim and the continuous decrease in Al outward in the rim. Plus signs represent jacobsite, open circles are galaxite, and filled squares are magnetite.

TABLE 3. Compositions of host, rim, and exsolved spinels, Sample VMNH no. 603

| | Exsolved Al-rich (cores) | Exsolved Fe-rich (haloes) | Reconst. exsolved | Host | Rim |
|--------------------------------|-----------------------------|------------------------------|----------------------|-------|-------|
| SiO ₂ | 0.05 | 0.03 | 0.03 | 0.06 | 0.04 |
| TiO ₂ | 0.09 | 1.59 | 1.19 | 0.73 | 0.87 |
| Al ₂ O ₃ | 46.96 | 11.62 | 21.09 | 21.52 | 6.93 |
| MgO | 1.84 | 0.30 | 0.71 | 0.46 | 0.18 |
| MnO | 29.44 | 28.74 | 28.93 | 30.14 | 27.04 |
| FeO | 3.54 | 4.76 | 4.43 | 3.74 | 4.76 |
| Fe ₂ O ₃ | 14.61 | 52.44 | 42.30 | 41.94 | 58.20 |
| ZnO | 3.77 | 0.37 | 1.28 | 0.48 | 0.31 |
| sum | 100.29 | 99.84 | 99.96 | 99.07 | 98.33 |
| Formula proportions* | | | | | |
| Fe ³⁺ | 0.330 | 1.419 | 1.088 | 1.086 | 1.642 |
| Fe ²⁺ | 0.089 | 0.143 | 0.126 | 0.108 | 0.149 |
| Ti | 0.002 | 0.043 | 0.031 | 0.019 | 0.025 |
| Al | 1.663 | 0.493 | 0.849 | 0.872 | 0.306 |
| Mg | 0.082 | 0.016 | 0.036 | 0.024 | 0.010 |
| Mn | 0.749 | 0.875 | 0.837 | 0.878 | 0.858 |
| Zn | 0.084 | 0.010 | 0.032 | 0.012 | 0.009 |
| jac | 9.1 | 59.9 | 44.6 | 45.0 | 69.6 |
| glx | 80.3 | 25.0 | 41.9 | 43.9 | 15.0 |
| mag | 10.6 | 15.1 | 13.5 | 11.1 | 15.5 |

Notes: Exsolved spinels reconstructed with 26.8 vol% Al-rich and 73.2 vol% Fe-rich exsolved spinel. This proportion was determined by modal analysis of BSE images (e.g., Fig. 6). Compare reconstructed exsolved spinel analysis with host spinel analysis. Jac, glx, and mag normalized to 100%.

* Based on three cations and four oxygen atoms.

tschermakite. Along with intermediate plagioclase (An₄₂), presence of this calcic amphibole indicates a calc-pelitic tendency of the schist. Sillimanite occurs as fibrolite in masses that may be interpreted texturally to be pseudomorphs after andalusite.

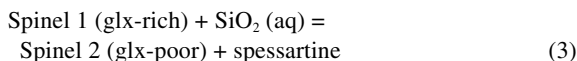
Fe-Mg exchange thermometry using garnet (alm₈py₇sp₆gr₆) and biotite (F/FM = 0.656) yields a *T* of 575 °C (Holdaway

2000) and GASP barometry using the same garnet as well as plagioclase (An_{42}) yields a P of 4.2 kbar (Holdaway in press). Using THERMOCALC (Holland and Powell 1998), the intersection of the grt-bt exchange and GASP net-transfer equilibria was calculated at 580 °C and 3.9 kbar. We therefore accept the conditions of regional metamorphism at the Hutter Mine as approximately 575 °C and 4 kbar. The P - T estimates are consistent with the position of the observed mineral assemblages on appropriate petrogenetic grids (cf., Spear 1993), and are very similar to those proposed by Winter and others (1981) for the Bald Knob Mn deposit.

Silica activity and diffusion in reaction zones

The lack of thermodynamic data for galaxite precludes the calculation of a quantitative silica activity profile for the reaction zone in VMNH no. 615. Nevertheless, it is possible to infer some aspects of silica behavior from the spinel compositions in the reaction zone.

First, the abrupt change to less-aluminous spinel at the initial appearance of garnet (Fig. 4) clearly reflects the crossing of a reaction boundary related to silica activity. Once this boundary is crossed, there is a continuous (and approximately linear) decrease in the galaxite content of the spinel, which drops to near zero well before the quartz-in boundary. A simple interpretation of this profile concludes that silica activity is (1) largely unbuffered (except in the narrow zone where it is buffered by tephroite + spinel + spessartine); (2) controlled over most of the zone by continuous reactions of the sort:



and (3) increases steadily throughout the reaction zone. We also infer from this data and from the presence of skarns elsewhere (e.g., VMNH no. 603), that during metamorphism of the Hutter Mine deposit, silica was largely redistributed as an aqueous species.

On the other hand, the boundary between the Fe-rich and the Mn-rich spinel (and silicates) regions in the VMNH no. 615 reaction zone is sharp. The molar variations of both Mn and Fe^{2+} in spinel with distance approximate sigmoidal curves like those typical of solid-state diffusion profiles (Fig. 4, compare with Albarede 1995, p. 432). This boundary is likely to approximate an initial lithologic boundary in this sample. Originally, this boundary probably separated quartz-bearing from quartz-free lithologies (i.e., carbonate from quartz-amphibolite). The current displacement of the quartz-in boundary away from its original location likely reflects solution and transport of silica across the interface.

Constraints from the stability relations of Mn oxides and spinels

Oxygen fugacity, at least in the manganosite-bearing sample at the time of manganosite formation, is tightly constrained: it must lie along the manganosite-hausmannite oxygen buffer. This places f_{O_2} well within the magnetite stability field (Huebner 1976) and is thus consistent with the presence of magnetite ore at the Hutter Mine. However, given the wide range of rock compositions and chemical mobility demonstrated here, it is

likely that there was substantial local variation in f_{O_2} , at least within the magnetite stability field.

In most of its natural occurrences, manganosite forms by decarbonation of Mn-rich carbonates (Huebner 1969, and references therein). At amphibolite-facies temperatures, this requires a low- f_{CO_2} fluid (Huebner 1969) (Fig. 7). We suggest that an H_2O -rich metamorphic fluid locally infiltrated the Mn-rich marble and led to the decarbonation of Mn- and Ca-Mn-carbonates via the decarbonation reaction:



Because of the lack of context for the manganosite-bearing sample, it is not possible to know how this reaction related to other reaction zone phenomena. However, manganosite stability certainly requires very low silica activity (Fig. 7). Therefore, any region where reaction 4 operated must differ in important respects from silicification zones found in (for example) VMNH no. 615 (Fig. 4, and discussion above).

On the other hand, the proposed miscibility gap in Mn-Al- Fe^{3+} spinels at Bald Knob (at $T = 575 \pm 40$ °C; Winter et al. 1981), combined with limited experimental work, could be interpreted to suggest that the near-complete miscibility observed at the Hutter Mine could reflect temperatures as high as 900 °C (Ishida et al. 1977). However, we can envision no realistic scenario whereby the Mn-rich rocks could have attained (and preserved evidence for) such high temperatures within their

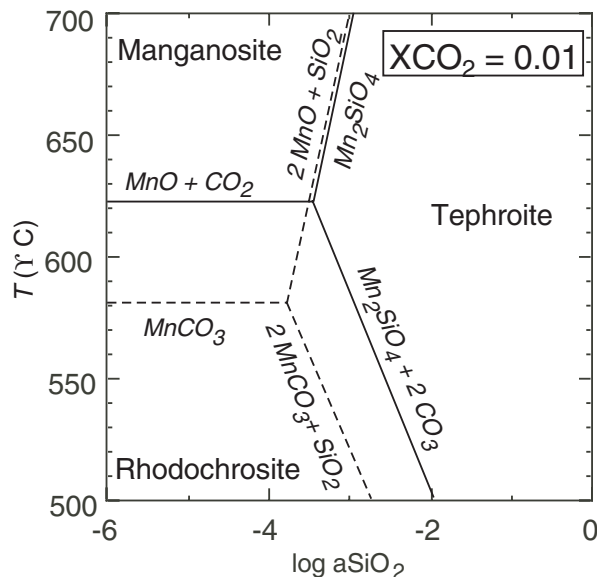


FIGURE 7. Stability of manganosite, tephroite, and rhodochrosite calculated using THERMOCALC (Holland and Powell 1998). SiO_2 is assumed to be a mobile, aqueous species. Fluid is 1% CO_2 , 99% H_2O . Solid line was calculated with activity of rhodochrosite in carbonate assumed equal to mole fraction rhodochrosite in carbonate ($C_{c55}R_{h45}$) from sample VMNH no. 598. Dashed line assumes pure rhodochrosite. A low- T solvus in the system MnCO_3 - CaCO_3 should result in a positive deviation from ideality, so the equilibrium curves for reactions involving rhodochrosite should lie between the dashed and solid lines. Lowering CO_2 in the fluid also enlarges the manganosite field.

amphibolite-facies regional metamorphic environment. It therefore appears that intermediate-composition Mn-spinel solid solutions must be stable at temperatures lower than previous work has indicated.

DISCUSSION

High-*T* miscibility in the Jacobsite-Hausmannite system

Curiously, there is another miscibility problem at the Hutter Mine of opposite and perhaps equal magnitude that concerns the coexistence of hausmannite and nearly pure jacobsite (96%; Table 1). Although most natural hausmannites are relatively pure, coexisting jacobsites typically contain substantial (e.g., 50%) dissolved hausmannite at moderate temperatures, according to Mason (1943a, 1943b).

The most obvious interpretation of coexisting, near end-member jacobsite with hausmannite at Hutter is that the two phases have thoroughly unmixed and equilibrated at low *T*. Such unmixing, however, typically produces characteristic intergrowth patterns ("vredenburgite": Mason 1943b), which are absent in VMNH no. 598. Furthermore, although hausmannite and jacobsite are found in contact with each other, they more commonly occur separately. In fact, of five thin sections of VMNH no. 598, all contain jacobsite and manganosite, but only two also contain hausmannite and only one of those contains large, rounded, hausmannite grains. In the limited context of what is known about the magnetite-hausmannite-jacobsite system, we have no explanation for the coexistence of essentially pure jacobsite and hausmannite, apparently in a high-temperature assemblage. One speculation is that the "jacobsite" in VMNH no. 598 contains substantially more Mn³⁺ than is required by stoichiometry and actually represents a magnetite-hausmannite solid solution. Recalculation of the jacobsite formula to maximize hausmannite yields a "spinel" that is about two parts magnetite to one part hausmannite. Detailed phase relations in the magnetite-hausmannite system were poorly known at the time of Mason's (1943a) review paper and largely remain so today. In fact, von Eckermann (1943) even suggested on the basis of crystal-structural data that hausmannite was not Mn²⁺Mn³⁺O₄ at all, but actually Mn⁴⁺Mn²⁺O₄. Mossbauer spectroscopy or similar techniques will likely be required to sort out this polyvalent system.

Low-*T* miscibility in the Mn-spinel series

The most straightforward interpretation of the Hutter Mine data is that the miscibility gaps in the jacobsite-magnetite and jacobsite-galaxite joins are small or absent, even at temperatures below 600 °C. However, this interpretation requires reconsideration of the Essene and Peacor (1983) Bald Knob data set. We argue that a series of compositional factors have conspired to create the appearance of a jacobsite-galaxite miscibility gap both at Bald Knob and, to a lesser extent, at the Hutter Mine.

First, the most aluminous spinels (*glx* > 70) at both the Hutter Mine and Bald Knob contain substantial Mg, Zn, and (at Bald Knob) Co, >5 mol% spinel + gahnite + Co-spinel in most cases (Essene and Peacor 1983) (Table 1). If these excess components have stabilized a second spinel phase at the Hutter Mine and at Bald Knob, the coexistence of the two spinels may not

be related to the galaxite-jacobsite two-phase region. A second possible mode of origin for the some of the aluminous spinels is that they formed during retrograde exsolution. Unequivocal exsolution features are seen in a few aluminous jacobsite grains at the Hutter Mine (see above and Figs. 2, 5, and 6). In fact, the aluminous exsolved spinels at the Hutter Mine are also enriched in Mg and Zn, whereas the Fe-rich exsolved spinels are enriched in Ti (Table 3). This observation suggests that these excess components may promote immiscibility along the nominal jacobsite-galaxite join.

As for the jacobsite-rich spinels, it is arguable that much of their compositional variation is a function of bulk composition, specifically silica activity. Bald Knob has essentially two lithologies, both Mn-rich: silica-poor carbonate-rich layers (where spinels are found), and quartz-rich rocks containing abundant Mn-pyroxenoids and spessartine (Simmons et al. 1981; Winter et al. 1981; Flohr 1992). All Bald Knob spinels for which analyses have been reported occur in rocks containing manganohumite or alleghanyite and lacking Mn-pyroxenoids and (with a single exception) spessartine (Essene and Peacor 1983). If reaction zones are present at the interface of silica-rich and silica-poor rocks at Bald Knob, no mineral analyses are specifically reported for them.

Most of the extensive compositional variation of Mn-spinels along the jacobsite-galaxite join at the Hutter Mine simply reflects the greater variability of silica content in rocks containing spinel. This effect is exemplified by spinel chemistry in reaction zones, some of which (e.g., VMNH no. 615, Fig. 2) exhibit at least as much variation in spinel composition as in the suite as a whole. Hutter Mine spinels lying in the apparent Bald Knob miscibility gap are simply reflecting the extended range of silica activity at the Hutter Mine compared to the essentially bimodal silica distribution at Bald Knob.

In summary, we interpret the differences in jacobsite-galaxite solid-solution behavior between the Hutter Mine and the Bald Knob locality as reflecting a combination of (1) the stabilization of a galaxite-rich second spinel phase by incorporation of Mg, Zn, and (at Bald Knob) Co; (2) retrograde exsolution (at least at the Hutter Mine), possibly promoted by excess Mg, Zn, and Ti; and (3) most importantly, differences in the range of silica activities at the two localities. Unless the galaxite-jacobsite and jacobsite-magnetite two-phase regions are highly asymmetric, it is unlikely that their crests lie above 600 °C.

ACKNOWLEDGMENTS

We thank Bill Henika of the Virginia Dept. of Mines, Minerals and Energy for alerting us to the work being done by VDMME at the Hutter Mine site and for his subsequent help and interest in the Hutter Mine minerals. Thanks also to Eric Essene and Steve Huebner for very careful and constructive reviews of the manuscript. This work has been supported by the Virginia Museum of Natural History.

REFERENCES CITED

- Albarede, F. (1995) *Introduction to Geochemical Modeling*, 543 p. Cambridge, New York.
- Beard, J.S. and Tracy, R.J. (1996) Contact granulites in the Smith River Allochthon, south-central Virginia. *Geological Society of America abstracts with program*, 28, Southeast Section.
- Carvalho III, A.V. and Sclar, C.B. (1988) Experimental determination of the ZnFe₂O₄-ZnAl₂O₄ miscibility gap with application to franklinite-gahnite exsolution intergrowths from the Sterling Hill zinc deposit, New Jersey. *Economic Geology*, 83, 1447-1452.
- Conley, J.F. (1985) *Geology of the Southwestern Virginia Piedmont*. Virginia Divi-

- sion of Mineral Resources Publication 59, 33 p.
- Conley, J.F. and Henika, W.S. (1973) Geology of the Snow Creek, Martinsville East, Price, and Spray Quadrangles, Virginia. Report of Investigations 33. Virginia Division of Mineral Resources, Charlottesville, 71 p.
- Dasgupta, S., Banerjee, H., Fukuoka, M., Bhattacharya, P.K., and Roy, S. (1990) Petrogenesis of metamorphosed manganese deposits and the nature of precursor sediments. *Ore Geology Reviews*, 5, 359–384.
- von Eckermann, H. (1943) Some remarks on the Fe_2O_3 - Mn_2O_3 system. *Geologiska Foreningen i Stockholm Forhandling*, 65, 258–262.
- Espenshade, G.H. (1954) Geology and Mineral Deposits of the James River-Roanoke River Manganese District, Virginia. United States Geological Survey Bulletin 1008, 155 p.
- Essene, E.J. and Peacor, D.R. (1983) Crystal chemistry and petrology of coexisting galaxite and jacobsite and other spinel solutions and solvi. *American Mineralogist*, 68, 449–455.
- Flohr, M.J.K. (1992) Geochemistry and origin of the Bald Knob manganese deposit, North Carolina. *Economic Geology* 87, 2023–2040.
- Furcron, A.S. (1935) James River Iron and Marble Belt, Virginia. Virginia Geological Survey Bulletin, 39, 124 p.
- Gates, A.E. and Speer, J.A. (1991) Allochemical retrograde metamorphism in shear zones: an example in metapelites, Virginia, USA. *Metamorphic Geology*, 9, 581–604.
- Ghiorso, M.S. and Sack, R.O. (1991) Thermochemistry of the oxide minerals. In P.H. Ribbe, Ed., *Oxide Minerals: Petrologic and Magnetic Significance*, 25, 221–264. Reviews in Mineralogy, Mineralogical Society of America, Washington, D.C.
- Glover, L., Speer, J.A., Russell, G.S., and Farrar, S.S. (1983) Ages of regional metamorphism and ductile deformation in the central and southern Appalachians. *Lithos*, 16, 223–245.
- Henika, W.S., Beard, J., Tracy, R., and Wilson, J.R. (2000) Structure and Tectonic Field Trip to the Eastern Blue Ridge and the Western Piedmont near Martinsville, Virginia: Virginia Minerals, 46, 1–32.
- Hill, R.J., Craig, J.R., and Gibbs, G.V. (1979) Systematics of the spinel structure type. *Physics and Chemistry of Minerals*, 4, 317–339.
- Holdaway, M.J. (2000) Application of new experimental and garnet Margules data to the garnet-biotite thermometer. *American Mineralogist*, 85, 881–892.
- (2001) Recalibration of the GASP geobarometer in light of recent garnet and plagioclase activity models and versions of the garnet-biotite geothermometer. *American Mineralogist*, 86, 1117–1129.
- Holland, T.J.B. and Powell, R. (1998) An internally consistent thermodynamic dataset for phases of petrologic interest. *Journal of Metamorphic Geology*, 16, 309–343.
- Huebner, J.S. (1967) Stability Relations of Minerals in the System Mn-Si-C-O, 279 p. Ph.D. Dissertation, Johns Hopkins University, Maryland.
- (1969) Stability relations of rhodochrosite in the system manganese-carbon-oxygen. *American Mineralogist*, 54, 457–481.
- (1976) The manganese oxides—a bibliographic commentary. In D. Rumble, Ed., *Oxide Minerals*, 3, SH1-SH17. Reviews in Mineralogy, Mineralogical Society of America, Washington, D.C.
- Ishida, K., Momoi, H., and Hirowatari, F. (1977) Hydrothermal synthesis of the jacobsite-galaxite join. *Kyushu Daigaku Rigakubu Kenkyu Hokoku, Chishitsugaku*, 12, 289–297.
- Kretz, R. (1983) Symbols for rock-forming minerals. *American Mineralogist*, 68, 277–279.
- Lindsley, D.H. (1991) Experimental studies of oxide minerals. In P.H. Ribbe, Ed., *Oxide Minerals: Petrologic and Magnetic Significance*, 25, 69–106. Reviews in Mineralogy, Mineralogical Society of America, Washington D.C.
- Marr, J.D. (1984) Geologic Map of the Pittsville and Chatham Quadrangles, Virginia. Virginia Division of Mineral Resources, Publication 49.
- Mason, B. (1943a) Mineralogical aspects of the system $\text{FeO-Fe}_2\text{O}_3\text{-MnO-Mn}_2\text{O}_3$. *Geologiska Foreningen i Stockholm Forhandling*, 65, 97–180.
- (1943b) Alpha-vredenburgite. *Geologiska Foreningen i Stockholm Forhandling*, 65, 263–270.
- McSween, H.Y. (1976) Manganese-rich ore assemblages from Franklin, New Jersey. *Economic Geology*, 71, 814–817.
- Pouchou, J.L. and Pichoir, F. (1985) “PAP” procedure for improved quantitative microanalysis. *Microbeam Analysis*, 20, 104–105.
- Simmons, W.B., Peacor, D.R., Essene, E.J., and Winter, G.A. (1981) Manganese minerals of Bald Knob, North Carolina. *Mineralogical Record*, 12, 167–171.
- Speer, F.S. (1993) *Metamorphic Phase Equilibria and Pressure-Temperature-Time Paths*, 799 p. Mineralogical Society of America, Washington, D.C.
- Watanabe, T., Yui, S., and Kato, A. (1970) Metamorphosed bedded manganese deposits of the Noda-Tamagawa Mine. In T. Tatsumi, Ed., *Volcanism and Ore Genesis*, p. 143–152. University of Tokyo Press, Tokyo.
- Watson, T.L. (1907) Mineral Resources of Virginia, 618 p. J.P. Bell, Lynchburg, Virginia.
- Winter, G.A., Essene, E.J., and Peacor, D.R. (1981) Carbonates and pyroxenoids from the manganese deposit near Bald Knob, North Carolina. *American Mineralogist*, 66, 278–289.

MANUSCRIPT RECEIVED JULY 3, 2001

MANUSCRIPT ACCEPTED JANUARY 17, 2002

MANUSCRIPT HANDLED BY WALTER E. TRZCIENSKI JR.